

WRQ-2, a gemcitabine prodrug, reverses gemcitabine resistance caused by hENT1 inhibition

Ruquan Wang^{1,§}, Yongliang Li^{2,§}, Jianjun Gao^{1,*}, Yepeng Luan^{2,*}

¹Department of Pharmacology, School of Pharmacy, Qingdao University Qingdao Medical College, Qingdao University, Qingdao, Shandong, China;

²Department of Medicinal Chemistry, School of Pharmacy, Qingdao University Qingdao Medical College, Qingdao University, Qingdao, Shandong, China.

SUMMARY Gemcitabine is widely used in the clinic as a first-line antitumor agent. However, intrinsic and acquired resistance hinders its wide clinical application. In this study, a gemcitabine prodrug nominated as WRQ-2 was designed and synthesized by conjugating gemcitabine with the indole-3-methanol analogue OSU-A9 through a carbamate linkage. WRQ-2 exhibited high cytotoxicity against six cancer cell lines (HeLa, A549, MDA-MB-231, HuH-7, MGC-803, and HCT-116) with IC₅₀ values in low micromolar range. WRQ-2 reversed the resistance of HeLa cells to gemcitabine caused by hENT1 inhibition. Compared to gemcitabine, WRQ-2 induced a higher degree of DNA damage and apoptosis in the presence of hENT1 inhibitor. Our study suggests that compound WRQ-2 is a potential gemcitabine prodrug and worth of further antitumor activity investigation.

Keywords Gemcitabine, prodrug, drug resistance, OSU-A9, cancer

1. Introduction

Pyrimidine nucleoside analogs are an important class of chemotherapeutic agents with excellent cytotoxic activity against a wide range of cancers (1,2). Gemcitabine (2',2'-difluoro-2'-deoxycytidine, dFdC) is one of the representative drugs which was first synthesized by Hertel *et al.* in 1988 and is the first-line drug for pancreatic cancer and non-small cell lung cancer since it was approved by the FDA in 1996 (3,4). Gemcitabine functions as a prodrug that needs to be activated intracellularly before exerting antitumor effect (5). Gemcitabine is transported into the cell mainly *via* human equilibrative nucleoside transporter 1 (hENT1) (6,7) and then, it is phosphorylated by deoxycytidine kinase (dCK) to gemcitabine monophosphate (dFdCMP), and dFdCMP is successively phosphorylated by nucleoside monophosphate and diphosphate kinase to gemcitabine diphosphate (dFdCDP) and gemcitabine triphosphate (dFdCTP) (8,9). dFdCTP can replace the site of deoxycytidine and competitively bind into the DNA strand which results in the cessation of DNA strand synthesis, DNA breakage and cell death (10,11). In addition, gemcitabine can lead to depletion of dNTPs pool by inhibiting cytidine-5'-triphosphate (CTP) synthase (12).

Although gemcitabine plays important roles in the clinical treatment of cancers, its wide use is greatly

hindered due to intrinsic or acquired drug resistance. There are three main mechanisms leading to drug resistance, (i) downregulation of dCK, the rate-limiting enzyme for the first step of phosphorylation, resulting in insufficient conversion to the dFdCDP and dFdCTP forms (13,14); (ii) lack of nucleoside transport proteins responsible for bringing gemcitabine into tumor cells, including hENT1 and concentrative nucleoside transporter 1 (CNT1), which makes it difficult for gemcitabine to enter tumor cells; (iii) overexpression of cytidine deaminase (CDA), which is able to metabolize gemcitabine to the inactive 2',2'-difluoro-2'-deoxyuridine (dFdU) (15). Therefore, there is an urgent need to improve the efficiency of gemcitabine. To overcome the problems of drug resistance and poor metabolic stability, prodrugs of gemcitabine with different structural features are widely developed *via* structural modification of either 4-amino or 5'-hydroxyl groups to attenuate drug resistance and improve efficiency (16,17).

Indole-3-carbinol (I3C) is a broadly existing phytochemical that has been proven in animal studies to prevent carcinogenic effects and inhibit the proliferation of human breast, colon, prostate, and endometrial cancer cells (18). Furthermore, mechanistic evidence suggests that I3C was able to induce growth arrest and apoptosis by regulating a broad range of signaling pathways associated with cell cycle regulation and survival (19,20). OSU-A9, an I3C analogue, possesses apoptosis-inducing

capacity which is much more potent than that of the parental I3C. In addition, OSU-A9 retains the pleiotropic potency of I3C against multiple signaling pathways associated with growth arrest and apoptosis, while normal cells are less sensitive (21).

On the other hand, in addition to using as monotherapy, gemcitabine has shown good synergistic effects in combination with other anticancer drugs such as kinase inhibitors (22,23) and histone deacetylase inhibitors (24,25). For example, in 2016, Jiang *et al.* combined gemcitabine and ubenimex to design novel interacting prodrugs, which released gemcitabine intracellularly and showed desirable cytotoxicity (26). As previously mentioned, 4-amino acids are affected by CDA metabolism, which reduces the efficacy of gemcitabine, and this challenge can be solved by modifying 4-amino group to construct prodrugs. The structures of 4-amino-based gemcitabine prodrugs mainly include amides and carbamates, which can be readily hydrolyzed in tumor cells to release free gemcitabine. Based on the results of existing studies, we designed and synthesized a novel gemcitabine prodrug, named as WRQ-2, to link OSU-A9 with the 4-amino group of gemcitabine through a carbamate bond. WRQ-2 displayed comparable antitumor activity to gemcitabine and attenuate the drug resistance (Figure 1).

2. Materials and Methods

2.1. Cell lines and culture

A549 (human lung cancer cell line), MDA-MB-231 (human breast cancer cell line), HuH-7 (human hepatoma cell line), and MGC-803 (human gastric cancer cell line) cells were cultured in Dulbecco's modified Eagle medium (DMEM, Gibco, Grand Island, NY, USA) supplemented with 10% fetal bovine serum. HeLa (human cervical cancer cell line) cells were cultured in modified Eagle medium (MEM, Gibco) supplemented with 10% fetal bovine serum. HCT-116 (human colorectal cancer cell line) cells were cultured in Iscove's modified Dulbecco's medium (IMDM, Gibco) supplemented with 10%

fetal bovine serum. These cells were obtained from the National Infrastructure of Cell Line Resource (Beijing, China).

2.2. Cell proliferation assay

Cancer cells inoculated in 96-well plates (5×10^3 per well) were exposed to the indicated drugs for 72 h. In the assay for gemcitabine (Energy Chemical, Shanghai, China) resistance, tumor cells were pre-incubated with dipyrindamole (10 μ M; Energy Chemical), which is a well-documented hENT1 inhibitor, three hours before exposure to various concentrations of WRQ-2 or gemcitabine for 72 h. Then, the medium was removed and the wells were washed with phosphate-buffered saline (PBS, Gibco). Fifteen microliters of 3-(4,5-dimethylthiazol-2-yl)-2,5-diphenyltetrazolium bromide (MTT; Sigma, St. Louis, MO, USA) were added to each well at a working concentration of 5 mg/mL. After 4 h incubation, the medium was removed and 150 μ L of DMSO was added to each well to dissolve the crystals. The absorbance was measured at 490 nm on a microplate reader (Tecon, Switzerland).

2.3. Cell apoptosis assay

Apoptosis rates were assessed using the Annexin V-FITC/PI apoptosis detection kit (Solarbio, Beijing, China) according to the manufacturer's instructions. HeLa cells were inoculated into 6-well tissue culture plates (4×10^5 cells/well). After 36 h of drug treatment, cells were collected, washed with PBS, and resuspended in 1 mL of binding buffer. Then, 5 μ L Annexin V-FITC and 5 μ L PI were added to the binding buffer and incubated for 15 min at room temperature and protected from light. Cells were analyzed by flow cytometry (Beckman Coulter, Brea, California, USA) within 1 hour.

2.4. Western blot

HeLa cells were seeded in a six-well transparent plate (5×10^5 cells/well). Different concentrations of compounds WRQ-2 or gemcitabine were added to cells followed by incubation for 24 h. PBS was utilized to harvest and wash the cells three times. After that, RIPA cell lysis buffer (Thermo Fisher Scientific, Waltham, Massachusetts, USA) was used to lyse the cells on ice for a half-hour, followed by centrifugation of the cell lysates at $12,000 \times g$ for 15 min at 4°C. After collecting the supernatant from the centrifuge, bicinchoninic acid (BCA, Thermo Fisher Scientific) protein assay was conducted to determine the protein concentration. Subsequently, sodium dodecyl sulfate-polyacrylamide gel electrophoresis (SDS-PAGE) was used to separate equal amounts of protein (20 μ g). After transferring the proteins to poly(vinylidene fluoride)

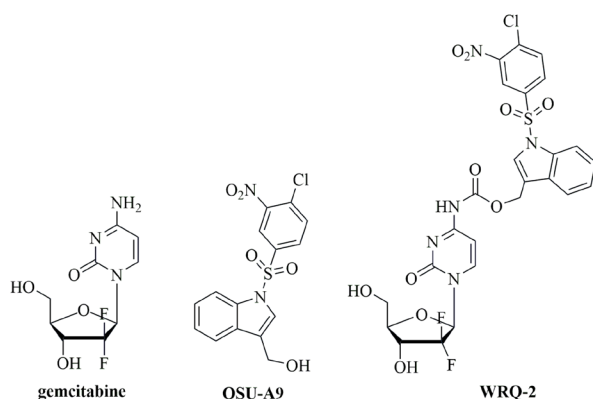


Figure 1. The structures of gemcitabine, OSU-A9, and the prodrug WRQ-2.

membranes, the proteins were blocked with 5% milk. After incubation with the primary antibody at 4°C for 12 h, the membranes were washed with TBST three times and incubated with horseradish peroxidase-conjugated secondary antibodies. The signal was visualized using an enhanced chemiluminescence reagent and detected by an ECL Western blotting detection system (Bio-Rad, Hercules, California, USA).

2.5. Statistical analyses

Data were expressed as mean \pm S.D. for three different determinations. Statistical significance was analyzed by one-way analysis of variance (ANOVA) followed by Dunnett's multiple range tests. The value of $p < 0.05$ was considered statistically significant. Statistical analysis was performed using the SPSS software.

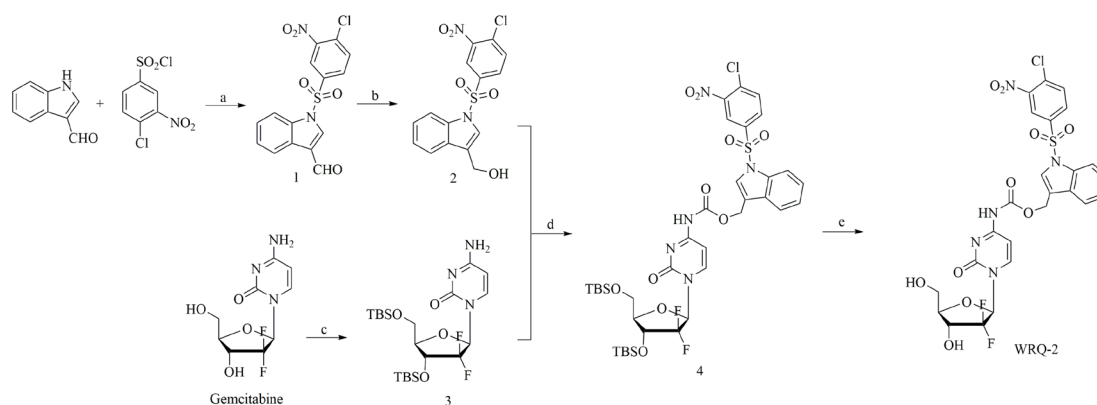
3. Results and Discussion

3.1. Chemistry

The synthesis route of WRQ-2 was outlined in Scheme 1. The compound 1 was obtained following the method reported by Che *et al.* (27). Two starting materials condensed under the condition of K_2CO_3 in anhydrous dichloromethane (DCM). The aldehyde group of compound 1 was reduced by $NaBH_4$ to afford the compound 2.

On the other hand, the double tert-butyldimethylsilyl (TBS) protected gemcitabine (compound 3) was obtained by using the method reported by Li, *et al.* (28). Compound 2 and 3 condensed to form the carbamate under the condition of triphosgene to give the compound 4. Finally, two TBS groups of compound 4 were removed by tetrabutylammonium fluoride (TBAF) in tetrahydrofuran (THF) to afford the targeted compound WRQ-2 (Appendix).

3.2. Cell proliferation inhibition



Scheme 1. Reagents and methods. (a) K_2CO_3 , anhydrous dichloromethane, room temperature, 20 h; (b) $NaBH_4$, MeOH, 0°C to room temperature, 12 h; (c) *t*-butyldimethylsilyl chloride, imidazole, anhydrous *N,N*-dimethylformamide, room temperature, 24 h; (d) triphosgene, triethylamine, anhydrous dichloromethane; (e) tetrabutylammonium fluoride, tetrahydrofuran, room temperature, 0.5 h.

The effect of WRQ-2 on cell viability against A549, MDA-MB-231, HuH-7, MGC-803, HeLa, and HCT-116 cells was determined using an MTT assay with gemcitabine as the positive control. WRQ-2 showed significant antiproliferative activity against all six tumor cells with IC_{50} values in the μM to the sub- μM range (Table 1), comparable to gemcitabine, which indicated that the carbamate bond of WRQ-2 might be cleaved intracellularly to release gemcitabine.

To investigate whether the compound WRQ-2 could reverse gemcitabine drug resistance suffering from low expression of hENT1, the cytotoxic effects of WRQ-2 and gemcitabine were examined by incubating HeLa cells with the hENT1 inhibitor dipyrindamole at a concentration of 10 μM . The results showed that the cytotoxicity of gemcitabine was significantly diminished when cells were pretreated with dipyrindamole, with IC_{50} values increased from 0.13 to 1.76 μM , by approximately 10-fold. In contrast, the cytotoxicity of WRQ-2 was not noticeably affected (0.17 μM for single treatment vs. 0.25 μM for co-treatment) which suggested that WRQ-2 may have the potential to reverse gemcitabine drug resistance caused by low expression of hENT1.

3.3. Induction of DNA damage in HeLa cells

The metabolite of gemcitabine can replace the site of deoxycytidine in the DNA strand by competitive

Table 1. Cytotoxic activity of compound WRQ-2 and gemcitabine on tumor cells

Tumor cells	<i>In vitro</i> cytotoxicity IC_{50} (μM)	
	WRQ-2	gemcitabine
HeLa	0.17 \pm 0.03	0.13 \pm 0.01
MGC-803	0.07 \pm 0.01	0.04 \pm 0.01
HCT-116	0.79 \pm 0.09	0.51 \pm 0.18
A549	1.05 \pm 0.09	0.82 \pm 0.06
HuH-7	1.43 \pm 0.11	0.93 \pm 0.13
MDA-MB-231	2.58 \pm 0.27	3.02 \pm 0.48

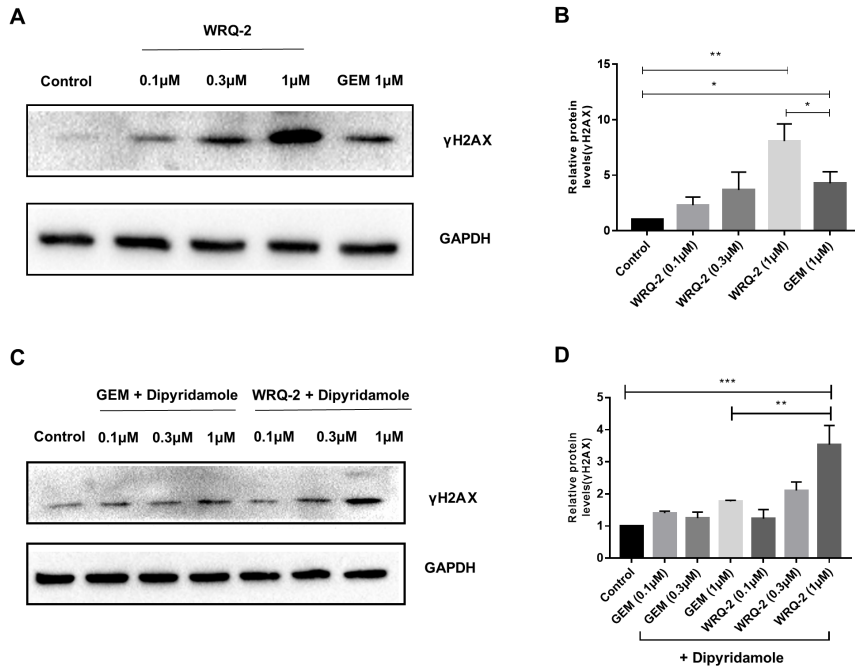


Figure 2. WRQ-2 and gemcitabine increase γH2AX protein expression in HeLa cells. (A, B) γH2AX expression was measured using western blot analysis in HeLa cells treated with WRQ-2 or gemcitabine for 24h. (C, D) Cells were pretreated with dipyridamole for 3 h and then exposed to gemcitabine or WRQ-2 for 24 h. γH2AX expression was measured using western blot analysis. GEM, gemcitabine. * $p < 0.05$, ** $p < 0.01$.

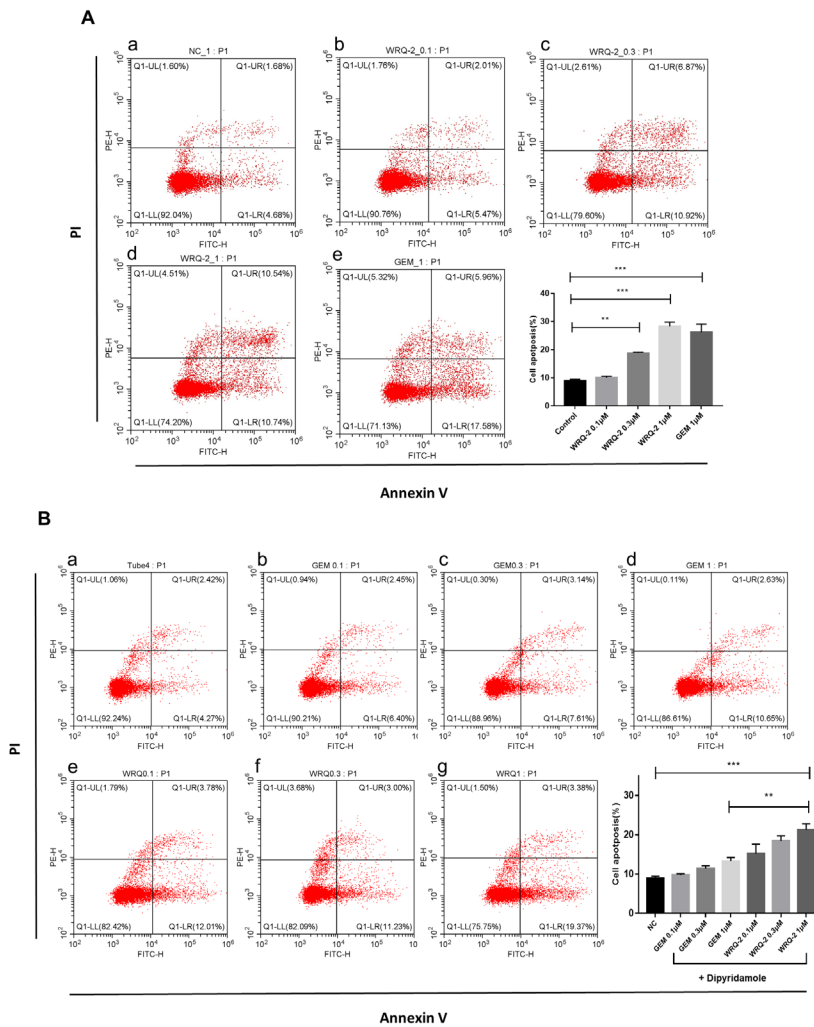


Figure 3. WRQ-2 and gemcitabine induce apoptosis in HeLa cells. (A) After incubation of cells with different concentrations of WRQ-2 or gemcitabine for 36 h, HeLa cells were stained with Annexin V/PI and the apoptosis rate was measured by flow cytometry analysis. a, vehicle; b, 0.1 μM WRQ-2; c, 0.3 μM WRQ-2; d, 1 μM WRQ-2; e, 1 μM gemcitabine. (B) HeLa cells were first pretreated with 10 μM dipyridamole for 3 h. After incubation with different concentrations of WRQ-2 or gemcitabine for 36 h, cells were stained with Annexin V/PI and the apoptosis rate was measured by flow cytometry analysis. a, vehicle; b, 0.1 μM gemcitabine + 10 μM dipyridamole; c, 0.3 μM gemcitabine + 10 μM dipyridamole; d, 1 μM gemcitabine + 10 μM dipyridamole; e, 0.1 μM WRQ-2 + 10 μM dipyridamole; f, 0.3 μM WRQ-2 + 10 μM dipyridamole; g, 1 μM WRQ-2 + 10 μM dipyridamole. GEM, gemcitabine. ** $p < 0.01$, *** $p < 0.001$.

incorporation into the DNA strand, resulting in the cessation of DNA strand synthesis and DNA damage. Accordingly, we examined the changes of the expression level of γ H2AX, a marker of DNA strand damage. As shown in Figures 2A and 2B, WRQ-2 significantly increased the level of γ H2AX, stronger than gemcitabine at the concentration of 1 μ M.

When cells were pretreated with dipyrindamole, WRQ-2 still significantly induced an elevated expression of γ H2AX, while gemcitabine induced much lower level (Figures 2C and 2D). These results suggested that WRQ-2 was capable of inducing more DNA damage than gemcitabine at the same dose in a hENT1 independent manner.

We noted that WRQ-2 increased the level of γ H2AX expression in HeLa cells, suggesting that WRQ-2 may be able to induce apoptosis in HeLa cells. We analyzed the apoptosis induced by WRQ-2 and gemcitabine in HeLa cell lines. HeLa cells were exposed to WRQ-2 (0.1, 0.3, or 1 μ M) and gemcitabine (1 μ M) at different concentrations for 36 h. Apoptosis of HeLa cells was subsequently detected by AnnexinV/PI staining and flow cytometry. As shown in Figure 3A, WRQ-2 could dose-dependently induced apoptosis in HeLa cells, and the degree of apoptosis was similar to that of gemcitabine at the concentration of 1 μ M. When cells were pretreated with dipyrindamole, the apoptosis-inducing effect of gemcitabine was inhibited, while WRQ-2 were less affected (Figure 3B). These results suggest that WRQ-2 can initiate apoptotic signaling in the presence of hENT1 inhibition.

4. Conclusion

In conclusion, a novel gemcitabine prodrug, WRQ-2, was rationally designed by conjugating with the antitumor compound OSU-A9. Compared with gemcitabine, WRQ-2 showed similar antiproliferative activity against six tumor cell lines with IC_{50} values in the μ M to the sub- μ M range. Furthermore, the cell proliferation inhibition capacity of WRQ-2 was not obviously affected by the inhibition of hENT1, whose low expression is one of the main reasons for gemcitabine resistance. In the presence of hENT1 inhibitor, the ability of gemcitabine to induce cellular DNA damage and apoptosis became weaker, while WRQ-2 was less affected, suggesting that WRQ-2 may enter cells in a hENT1 independent manner to exert antitumor effects. These results suggest that WRQ-2 is a promising gemcitabine prodrug that deserves further preclinical antitumor evaluation.

Funding: None.

Conflict of Interest: The authors have no conflicts of interest to disclose.

References

1. Robins RK. The potential of nucleotide analogs as inhibitors of retroviruses and tumors. *Pharm Res.* 1984; 1:11-18.
2. Gesto DS, Cerqueira NMFS, Fernandes PA, Ramos MJ. Gemcitabine: a critical nucleoside for cancer therapy. *Curr Med Chem.* 2012; 19:1076-1087.
3. Hertel LW, Boder GB, Kroin JS, Rinzel SM, Poore GA, Todd GC, Grindey GB. Evaluation of the antitumor activity of gemcitabine (2',2'-difluoro-2'-deoxycytidine). *Cancer Res.* 1990; 50:4417-4422.
4. Eckel F, Schneider G, Schmid RM. Pancreatic cancer: A review of recent advances. *Expert Opin Investig Drugs.* 2006; 15:1395-1410.
5. Fukunaga AK, Marsh S, Murry DJ, Hurley TD, McLeod HL. Identification and analysis of single-nucleotide polymorphisms in the gemcitabine pharmacologic pathway. *Pharmacogenomics J.* 2004; 4:307-314.
6. Heinemann V, Xu YZ, Chubb S, Sen A, Hertel LW, Grindey GB, Plunkett W. Cellular elimination of 2',2'-difluorodeoxycytidine 5'-triphosphate: A mechanism of self-potential. *Cancer Res.* 1992; 52:533-539.
7. Mackey JR, Mani RS, Selner M, Mowles D, Young D, Belt JA, Crawford CR, Cass CE. Functional nucleoside transporters are required for gemcitabine influx and manifestation of toxicity in cancer cell lines. *Cancer Res.* 1998; 58:4349-4357.
8. Ueno H, Kiyosawa K, Kaniwa N. Pharmacogenomics of gemcitabine: can genetic studies lead to tailor-made therapy? *Br J Cancer.* 2007; 97:145-151.
9. Dubey RD, Saneja A, Gupta PK, Gupta PN. Recent advances in drug delivery strategies for improved therapeutic efficacy of gemcitabine. *Eur J Pharm Sci.* 2016; 93:147-162.
10. Huang P, Chubb S, Hertel LW, Grindey GB, Plunkett W. Action of 2',2'-difluorodeoxycytidine on DNA synthesis. *Cancer Res.* 1991; 51:6110-6117.
11. Yuan YG, Peng QL, Gurunathan S. Silver nanoparticles enhance the apoptotic potential of gemcitabine in human ovarian cancer cells: combination therapy for effective cancer treatment. *Int J Nanomedicine.* 2017; 12:6487-6502.
12. Plunkett W, Huang P, Xu YZ, Heinemann V, Grunewald R, Gandhi V. Gemcitabine: Metabolism, mechanisms of action, and self-potential. *Semin Oncol.* 1995; 22:3-10.
13. Heinemann V, Hertel LW, Grindey GB, Plunkett W. Comparison of the cellular pharmacokinetics and toxicity of 2',2'-difluorodeoxycytidine and 1-beta-D-arabinofuranosylcytosine. *Cancer Res.* 1988; 48:4024-4031.
14. Gandhi V, Plunkett W. Modulatory activity of 2',2'-difluorodeoxycytidine on the phosphorylation and cytotoxicity of arabinosyl nucleosides. *Cancer Res.* 1990; 50:3675-3680.
15. Mini E, Nobili S, Caciagli B, Landini I, Mazzei T. Cellular pharmacology of gemcitabine. *Ann Oncol.* 2006; 17 (Suppl 5):v7-12.
16. Hong S, Fang Z, Jung HY, Yoon JH, Hong SS, Maeng HJ. Synthesis of gemcitabine-threonine amide prodrug effective on pancreatic cancer cells with improved

- pharmacokinetic properties. *Molecules*. 2018; 23:2608-2608.
17. Moysan E, Bastiat G, Benoit JP. Gemcitabine versus modified gemcitabine: a review of several promising chemical modifications. *Mol Pharm*. 2013; 10:430-444.
 18. Bai LY, Weng JR, Chiu CF, Wu CY, Yeh SP, Sargeant AM, Lin PH, Liao YM. OSU-A9, an indole-3-carbinol derivative, induces cytotoxicity in acute myeloid leukemia through reactive oxygen species-mediated apoptosis. *Biochem Pharmacol*. 2013; 86:1430-1440.
 19. Sarkar FH, Li Y. Indole-3-carbinol and prostate cancer. *J Nutr*. 2004; 134:3493S-3498S.
 20. Aggarwal BB, Chikawa H. Molecular targets and anticancer potential of indole-3-carbinol and its derivatives. *Cell Cycle*. 2005; 4:1201-1215.
 21. Weng JR, Tsai CH, Kulp SK, Wang D, Lin CH, Yang HC, Ma Y, Sargeant A, Chiu CF, Tsai MH, Chen CS. A potent indole-3-carbinol derived antitumor agent with pleiotropic effects on multiple signaling pathways in prostate cancer cells. *Cancer Res*. 2007; 67:7815-7824.
 22. Infante JR, Hollebecque A, Postel-Vinay S, *et al*. Phase I study of GDC-0425, a checkpoint kinase 1 inhibitor, in combination with gemcitabine in patients with refractory solid tumors. *Clin Cancer Res*. 2017; 23:2423-2432.
 23. Medinger M, Dreves J. Receptor tyrosine kinases and anticancer therapy. *Curr Pharm Des*. 2005; 11:1139-1149.
 24. Qiao Z, Ren S, Li W, Wang X, He M, Guo Y, Sun L, He Y, Ge Y, Yu Q. Chidamide, a novel histone deacetylase inhibitor, synergistically enhances gemcitabine cytotoxicity in pancreatic cancer cells. *Biochem Biophys Res Commun*. 2013; 434:195-101.
 25. Cai MH, Xu XG, Yan L, Sun Z, Ying Y, Wang BK, Tu YX. Depletion of HDAC1, 7 and 8 by histone deacetylase inhibition confers elimination of pancreatic cancer stem cells in combination with gemcitabine. *Sci Rep*. 2018; 8:1621.
 26. Jiang Y, Hou J, Li X, Huang Y, Wang X, Wu J, Zhang J, Xu W, Zhang, Y. Discovery of a novel chimeric ubenimex-gemcitabine with potent oral antitumor activity. *Bioorg Med Chem*. 2016; 24:5787-5795.
 27. Che Z, Zhang S, Shao Y, Fan L, Xu H, Yu X, Zhi X, Yao X, Zhang R. Synthesis and quantitative structure-activity relationship (QSAR) study of novel N-arylsulfonyl-3-acylindole arylcarbonyl hydrazone derivatives as nematocidal agents. *J Agric Food Chem*. 2013; 61:5696-5705.
 28. Li X, Hou Y, Meng X, Ge C, Ma H, Li J, Fang J. Selective activation of a prodrug by thioredoxin reductase providing a strategy to target cancer cells. *Angew Chem Int Ed Engl*. 2018; 57:6141-6145.

Received September 19, 2022; Revised December 5, 2022; Accepted December 6, 2022.

[§]These authors contributed equally to this work.

*Address correspondence to:

Yepeng Luan, Department of Medicinal Chemistry, School of Pharmacy, Qingdao University Qingdao Medical College, Qingdao University, Qingdao, Shandong, China.
E-mail: luanqdu@sina.com

Jianjun Gao, Department of Pharmacology, School of Pharmacy, Qingdao University Qingdao Medical College, Qingdao University, Qingdao, Shandong, China.
E-mail: gaojj@qdu.edu.cn

Released online in J-STAGE as advance publication December 16, 2022.

Appendix

For experimental work, chemical reagents and solvents are purchased from Energy Chemical and were used directly without any purification. The purity of the compounds was confirmed by thin-layer chromatography (TLC). Spots were visualized under ultraviolet lamp. ¹H NMR spectra in DMSO or CDCl₃ solution were respectively recorded at CDRI, Lucknow on NMR spectrometer (400 MHz, Bruker-400 Ultra shield TM) using TMS [(CH₃)₄Si] as internal standard. Splitting patterns are nominated as follows: s, singlet; d, doublet; t, triplet; m, multiplet. Mass spectra were recorded at CDRI, Lucknow on Mass spectrometer (Waters Synapt).

1-((4-chloro-3-nitrophenyl)sulfonyl)-1H-indole-3-carbaldehyde (1)

Indole-3-carbaldehyde (1 g, 6.8 mmol, 1.0 eq.) and 4-chloro-3-nitrobenzenesulfonyl chloride (3.52 g, 13.6 mmol, 2.0 eq.) were mixed in dry DCM. To this solution was added of K₂CO₃ (2.84 g, 20.4 mmol, 3.0 eq.). The mixture was refluxed for 20 h. The crude was purified by PE : EtOAc = 10:1 to obtain compound 1 2.2 g with yield of 88%. ¹H NMR (400 MHz, CDCl₃) δ: 10.13 (s, 1H), 8.47 (d, *J* = 2.5 Hz, 1H), 8.30 (d, *J* = 8.0 Hz, 1H), 8.18 (s, 1H), 8.06 (dd, *J* = 8.5 Hz, 2.5 Hz, 1H), 7.94 (d, *J* = 8.5 Hz, 1H), 7.72 (d, *J* = 8.5 Hz, 1H), 7.46-7.49 (m, 1H), 7.40-7.43 (m, 1H). EI-MS (*m/z*) Calcd for C₁₅H₁₀ClN₂O₃S⁺ [M+H]⁺ 365, found: 365.

(1-((4-chloro-3-nitrophenyl)sulfonyl)-1H-indol-3-yl)methanol (2)

Compound 1 (2 g, 5.4 mmol, 1.0 eq.) was dissolved in MeOH at 0°C, To this solution was added of NaBH₄ (0.2 g, 5.4 mmol, 1.0 eq.). After the mixture was stirred at 0 °C for 30 min, it was transferred to room temperature and stirred for 12 h. After extraction with EtOAc, concentrate solvent *in vacuo* to obtain compound 2 (1.95 g, 97%) which was used in the next step without purification. ¹H NMR (400 MHz, CDCl₃) δ: 8.74 (d, *J* = 2.2 Hz, 1H), 8.25 (dd, *J* = 8.6, 2.2 Hz, 1H), 7.99 (dd, *J* = 8.4, 6.3 Hz, 2H), 7.71-7.64 (m, 2H), 7.39 (t, *J* = 7.4 Hz, 1H), 7.31 (t, *J* = 7.4 Hz, 1H), 5.18 (t, *J* = 5.4 Hz, 1H), 4.62 (d, *J* = 5.4 Hz, 2H). EI-MS (*m/z*) Calcd for C₁₅H₁₂ClN₂O₃S⁺ [M+H]⁺ 367, found: 367.

4-amino-1-((2R,4R,5R)-4-((tert-butyldimethylsilyloxy)-5-(((tert-butyldimethylsilyloxy)methyl)-3,3-difluorotetrahydrofuran-2-yl)pyrimidin-2(1H)-one (3)

Gemcitabine (1 g, 3.8 mmol, 1.0 eq.) was dissolved in 25

mL of DMF. To this solution was added of imidazole (0.78 g, 11.4 mmol, 3.0 eq.) and of TBSCl (1.5 g, 9.5 mmol, 2.5 eq.). The mixture was stirred at 25°C for 24 h. The crude was purified by EtOAc : PE = 3:1 to obtain compound 4 (1.74g, 93%). ¹H NMR (400 MHz, DMSO-d⁶) δ 7.54 (d, *J* = 7.5 Hz, 1H), 7.41 (d, *J* = 4.0 Hz, 2H), 6.17 (t, *J* = 8.0 Hz, 1H), 5.77 (d, *J* = 7.5 Hz, 1H), 4.31 (dd, *J* = 20.7, 12.2 Hz, 1H), 3.95- 3.88 (m, 2H), 3.77 (dd, *J* = 12.1, 2.9 Hz, 1H), 0.89 (d, *J* = 6.5 Hz, 18H), 0.13-0.06 (m, 12H). EI-MS (m/z) Calcd for C₂₁H₄₀F₂N₃O₄Si₂⁺ [M+H]⁺ 492, found: 492.

(1-((4-chloro-3-nitrophenyl)sulfonyl)-1H-indol-2-yl)methyl (1-((1R,3R,4R)-3-((tert-butyldimethylsilyl)oxy)-4-(((tert-butyldimethylsilyl)oxy)methyl)-2,2-difluorocyclopentyl)-2-oxo-1,2-dihydropyrimidin-4-yl)carbamate (4)

A solution of triphosgene (134 mg, 0.45 mmol, 1.0 eq.) in dry DCM (5 mL) was added dropwise to a stirred solution of compound 3 (555 mg, 1.13 mmol, 2.5 eq.) and anhydrous Et₃N (313 μL, 2.25 μmol, 5.0 eq.) in dry DCM (10 mL) and stirred at 20°C for 2 h. A solution of compound 2 (414 mg, 1.13 mmol, 2.5 eq.) in dry DCM (5 mL) was added dropwise, and the solution stirred at 20°C for 24 h. The reaction mixture was condensed and the residue purified by chromatography, eluting with PE/EtOAc (v/v = 1:2) to get the pure compound 4. Yield: (380 mg, 38%) as a colorless oil. ¹H NMR (400 MHz, DMSO-d⁶) δ 8.66 (d, *J* = 2.2 Hz, 1H), 8.19 (dd, *J* = 8.6, 2.3

Hz, 1H), 7.96-7.88 (m, 4H), 7.63 (d, *J* = 7.8 Hz, 1H), 7.34 (t, *J* = 7.8 Hz, 1H), 7.25 (t, *J* = 7.8 Hz, 1H), 7.02 (d, *J* = 7.5 Hz, 1H), 6.11 (t, *J* = 7.3 Hz, 1H), 5.24 (s, 2H), 4.33-4.22 (m, 1H), 3.90-3.87 (m, 2H), 3.71 (dd, *J* = 12.2, 2.8 Hz, 1H), 0.81 (s, 9H), 0.79 (s, 9H), 0.01-0.00 (m, 12H). EI-MS (m/z) Calcd for C₃₇H₄₉ClF₂N₅O₁₀SSi₂⁺ [M+H]⁺ 884, found: 884.

(1-((4-chloro-3-nitrophenyl)sulfonyl)-1H-indol-2-yl)methyl (1-((1R,3R,4R)-2,2-difluoro-3-hydroxy-4-(hydroxymethyl)cyclopentyl)-2-oxo-1,2-dihydropyrimidin-4-yl)-14-azanecarboxylate (WRQ-2)

Compound 4 (88.3 mg, 0.1 mmol, 1.0 eq.) was dissolved in 5 mL THF, TBAF (1.0 M in THF, 300 μL, 3.0 eq.) was added and the mixture reacted at room temperature for 30 min. After the reaction, the solvent was concentrated in vacuum and the crude product was purified by DCM: MeOH = 20:1 to obtain the final product WRQ-2 as a white solid (60.3 mg, 92 %). ¹H NMR (400 MHz, DMSO-d⁶) δ 8.40 (d, *J* = 2.6 Hz, 1H), 8.25 (d, *J* = 7.7 Hz, 1H), 7.95-7.93 (m, 2H), 7.80 (dd, *J* = 9.1, 2.6 Hz, 1H), 7.71 (d, *J* = 7.8 Hz, 1H), 7.40 (t, *J* = 7.4 Hz, 1H), 7.31 (t, *J* = 7.4 Hz, 1H), 7.12 (d, *J* = 7.6 Hz, 1H), 6.92 (d, *J* = 9.1 Hz, 1H), 6.33 (brs, 1H), 6.16 (t, *J* = 7.4 Hz, 1H), 5.35 (s, 2H), 4.20 (dd, *J* = 21.2, 12.7 Hz, 1H), 3.89 (dt, *J* = 8.5, 2.9 Hz, 1H), 3.83-3.80 (m, 1H), 3.66 (dd, *J* = 12.7, 3.5 Hz, 1H). EI-MS (m/z) Calcd for C₂₅H₂₁ClF₂N₅O₁₀S⁺ [M+H]⁺ 656, found: 656.